Dendritic [Ca^{2+}] Dynamics in the Presence of Immobile Buffers and of Dyes

M. Maravall, Z.F. Mainen, K. Svoboda

Cold Spring Harbor Laboratory, Cold Spring Harbor, NY 11724, USA
maravall@cshl.org, zach@cshl.org, svoboda@cshl.org

Abstract. We present a reaction-diffusion model of [Ca^{2+}] regulation in neuronal dendrites, in the presence of high-affinity indicator and endogenous buffers. We investigate the applicability of equilibration assumptions for a slow, NMDAR-like source, present an analytical solution to the system in linear approximation, and discuss a possible scheme for extending this approximation's applicability. We obtain data on spatial Ca^{2+}spread that suggest that dendritic Ca^{2+}signals of NMDAR origin can be localized to $2 - 3\mu$m with no need for differential buffering or spines. Finally, we show that the difficulties presented by dye saturation may be circumvented by using fluorescence tails as a probe of [Ca^{2+}] peaks.

1 Introduction

Dendrites constitute the physical pathway through which information flows into a neuron. Dendritic calcium links changes in membrane polarization and neurotransmitter receptor activation to biochemical cell function. Thus dendritic calcium measurements, often involving fluorescent imaging microscopy, are vital to an understanding of neuronal computation [1].

When fluorescent dyes are introduced in a cell to enable calcium imaging, their chemical binding to Ca^{2+}competes with the homeostatic mechanisms that are naturally present in neurons. The dyes perturb experimental Ca^{2+}mobilities and thus peaks and durations of calcium transients. These effects depend not just on the relative driving forces of the different mechanisms, but also on the relative timescales on which they occur. When some of the interactions occur on timescales sufficiently quick compared to the others, they can be assumed to act independently of their slower counterparts, and can thus be treated separately. For instance, sometimes all chemical buffering can be considered to equilibrate locally on the timescales on which diffusion and extrusion operate. This is true in particular for homogeneous immobile buffer configurations, and for situations where the dominant buffers are fast. In these cases the coupling between the chemical kinetics and those of the other processes, and among the kinetics of the different chemical processes themselves, is minimal.

However, imaging dyes themselves alter the equilibrium properties of the Ca^{2+}-buffer complex. This is particularly true for high-affinity fluorophores such

as Fura 2 or the Ca^{2+}-(green, crimson, etc.) family of dyes, due to the slow off rates intrinsic to their affinities: equilibrium can be substantially slowed down compared to the cell's natural state [2]. Nonetheless, experimental data on Ca^{2+}transients are usually analyzed assuming that equilibrium does indeed occur in the dendritic shaft, because otherwise quantitative estimation becomes intractable.

The timescale of the source itself also contributes to determining whether equilibrium occurs. The more gradually Ca^{2+}enters a cell, the more it is available for distribution among buffers: a quick source, say an action potential, gives slow buffers little chance to take up ions before they are sequestrated by the faster buffers and perhaps by extrusion. This crucial aspect of binding has often been neglected in modelling efforts because of the use of unrealistically fast (instantaneous) or, conversely, of fixed sources. Here we consider source timescales that represent an NMDAR-dominated postsynaptic Ca^{2+}influx, and observe the effect of a varying source timescale on equilibrium.

When equilibrium does apply, Ca^{2+}mobility is determined by an effective diffusion constant dependent on the other buffers' properties as well. For instance, fixed endogenous buffer has the effect of greatly decreasing mobility, making diffusion much slower without greatly altering its properties: compared to free calcium diffusion, one has a slower but not qualitatively different phenomenon. The mathematical reflection of this effective diffusion is a one-equation description of the Ca^{2+}problem [3–5] which simplifies the modelling greatly. We give a solution of this equation for exponential NMDAR-like sources, valid for the case where (equilibrium) $[Ca^{2+}]$ is small compared to the buffers' dissociation constants. Unfortunately this parameter range is not very large. However, by means of an interpolative scheme we find that it is possible to extend the solution intuitively, giving an effective description of the equilibrated problem [5–8] and of the natural temporal and spatial scales on which Ca^{2+}homeostasis unfolds.

We also point out under what circumstances the insights that this approximation provides are valid even under borderline equilibrium. For instance, calcium spreads (and so spatial profiles) and peaks are greatly influenced by the presence of dye as opposed to only immobile buffers, and are consequently much more subject to nonequilibrium effects. However, the durations and times to peak of the $[Ca^{2+}]$ transients are comparatively unaffected [9]. We plot the results of calcium reaction-diffusion simulations in several useful approximations, and provide examples of all of these aspects of the problem.

Models, methods, approximations. Our model is described by the equation

$$\frac{\partial[Ca^{2+}]}{\partial t} = D_{Ca}\nabla^2[Ca^{2+}] - k_+^F[Ca^{2+}](F_T - [FCa]) + k_-^F[FCa] \qquad (1)$$
$$-k_+^B[Ca^{2+}](B_T - [BCa]) + k_-^B[BCa] - \Gamma([Ca^{2+}] - C_0) + J_0 f(x)g(t)$$

and similar ones describing the dynamics of B (the internal buffer) and F (the fluorophore). The terms on the right-hand side represent, respectively, diffusion, chemical binding kinetics, and (only for free Ca^{2+}) an extrusion decay term

governed by the constant Γ (where C_0 is the resting [Ca^{2+}]). The source term, parameterized by J_0 and the functions $(f(x), g(t))$, represents an NMDAR-like Ca^{2+}influx.

Experimentally, neither we nor other groups [6–9] have detected significant presence of mobile intrinsic buffers in pyramidal neuron dendrites. We thus considered a fast immobile buffer as the only intrinsic one present.

Dendritic geometry was approximated as a thin cylinder stretching over a short distance on either side of the source: enough to cover Ca^{2+}mobility over hundreds of milliseconds and to allow for simple boundary conditions at infinity to apply. The parameter J_0 represents the peak Ca^{2+}current density flowing into the dendrite. Functions $f(x)$ and $g(t)$ give the spatial dependence and time course of the influx. In the absence of more detailed data, the spatial profile can be modelled by a step function or Gaussian: we used both, and checked that the results' qualitative behavior was unaffected by this arbitrary choice. NMDA channel timecourses are generally modelled as either an alpha function or a double exponential with rise time much shorter than decay, which is on the order of 300ms. (The peak is reached after around $10 - 20$ms.) We did not find that using two temporal parameters was worthwhile at the level of fidelity to data we could aspire to maintain, so used a single decaying exponential in our simulations. The effect of using a single exponential and thus neglecting the shorter, rising, timecourse was to overestimate the decay timecourse by a small amount.

We computed peak current according to a minimal set of assumptions. First, we considered the case of possible dendritic spineless Ca^{2+} "hot spots": there is evidence (from our data and others') of NMDAR-like calcium influx events in parts of the dendrite with no observed spines. This, coupled to the existence of NMDA channels in shafts and to the fact that experimental data often fail to distinguish between spines and their neighboring shafts, justified a first approximation neglecting the complications of spine geometry. Because the Ca^{2+}current in this approximation is much higher than through a spine, the results thus obtained constituted lower bounds for localization, upper bounds for transient peaks and saturation, and lower bounds for the onset of equilibrium. Therefore all approximations involving equilibrium, to be discussed below, should apply to dendritic Ca^{2+}currents from spines if they apply to "hot-spot" currents. Estimates used our own whole-cell clamp data and also previous results on fractional Ca^{2+}currents (see [12] for references). To cast the current as a volume density we needed an estimate of the volume into which flow occurred: the region was a dendritic "slice", comprising the shaft's entire width and a length equal to the distance over which ions might spread on a fast timescale. This was set at around 1 μm, coinciding with other modelling estimates [9]. Final peak current estimate was around $J_0 \sim 5\mu\mathrm{M\,ms}^{-1}$; we let exact values be susceptible to free variation.

As for clearance, all mechanisms beyond fast buffering and diffusion were included in a single term, with available experimental evidence not justifying a more complicated treatment. In the absence of evidence to the contrary, we

assumed homogeneous distributions of extrusion and uptake mechanisms. This in turn justified the use of a one-dimensional longitudinal diffusion model. (Because no evidence for dendritic domains with varying calcium selectivity has been reported, inhomogeneous immobile buffer distributions were also unnecessary.) Based both on our own data and on similar experiments by other authors [6–9], we also neglected calcium-induced calcium release. The possible action of stores was restricted to uptake. Given all this, a good model for clearance was then provided by a minimal description of sequestration and pumping. using an effective Michaelis-Menten equation (see e.g. [10]). A leakage term [10] compensating for pump action at the resting steady state was also included. Because pump dissociation constants K_D^{p} are much larger than normal calcium concentrations, the resulting overall Michaelis-Menten clearance term could be approximated as

$$\left.\frac{\partial[\mathrm{Ca}^{2+}]}{\partial t}\right|_{\mathrm{ext}} + \left.\frac{\partial[\mathrm{Ca}^{2+}]}{\partial t}\right|_{\mathrm{lk}} \approx -\frac{V_{\mathrm{p}}}{K_D^{\mathrm{p}}}([\mathrm{Ca}^{2+}]-[\mathrm{Ca}^{2+}]_0) \equiv -\Gamma([\mathrm{Ca}^{2+}]-[\mathrm{Ca}^{2+}]_0). \quad (2)$$

Other mechanisms for internal uptake would also have comparatively high dissociation constants and so can be included as additional subtractive terms in this equation, again compensated for in the steady state. Particular values of Γ have been estimated [8] by computing effective time courses of Ca^{2+}transients as a function of dye concentration, and extrapolating down to zero dye capacity: in our notation, $\Gamma = 2.04 \pm 0.74\ \mathrm{ms}^{-1}$, which applies to our case given the similarities in experimental setup and dendritic model used. (The particular value chosen for many of our simulations was $\Gamma = 2.5$, although others were also used.)

The system was simulated using the Neuron software package [13], and could also be simplified according to a sequence of approximations. First, when the timescales involved in buffering are very fast compared to natural diffusion and extrusion time courses (which are of the order of 10ms), all chemical reactions can be assumed to be in equilibrium on those scales. (Since the different buffering processes interact with each other, the timescale which must be considered is the slowest one on which Ca^{2+}ions are interchanged between species [2].) Although nonequilibrium effects can be highly important —for instance, after single action potential stimulation [2, 11]—, our findings suggest that the system discussed here was close to local equilibration (see below). This justified use of the equilibrium approximation as a tool, although its validity should be verified in each specific case.

Under this approximation the full set of equations can be replaced by a single one, which describes an effective dynamics for free calcium with diffusive and decay terms [6, 3]. The diffusion coefficient involved is dependent on buffer capacities, which in turn are functions of Ca^{2+}concentration. In addition to this nonlinear "diffusion", there is an additional nondiffusive, nonlinear Ca^{2+}sink term, quadratic in the spatial gradient:

$$\kappa_T \frac{\partial C}{\partial t} = D_T \frac{\partial^2 C}{\partial x^2} - \frac{2}{K_D^F + C}\left(\frac{\partial C}{\partial x}\right)^2 - \Gamma(C - C_0) + J_0 f(x) g(t), \quad (3)$$

with $C \equiv [\mathrm{Ca}^{2+}]$, $D_T \equiv D_{\mathrm{Ca}} + \kappa_{\mathrm{B}} D_{\mathrm{B}} + \kappa_{\mathrm{F}} D_{\mathrm{F}}$ and $\kappa_T \equiv 1 + \kappa_B + \kappa_F$.

Often, the squared gradient term is quite small. It can then be neglected, giving rise to approximately diffusive behavior with the concentration-dependent diffusion constant given.

Finally, the dependencies on concentration through D_T and κ_T can be neglected in two limits within which the equation becomes linear and analytically solvable: in these, each buffer must either be saturated or else its dissociation constant must be much higher than the concentration of unbound calcium at equilibrium. The latter situation always applies to binding to endogenous buffers, since their effective dissociation constant is very high. Binding to the dye can span the range from one limit to the other, depending on calcium influx involved and on fluorophore characteristics. Thus the linear approximation's quality can vary dramatically. However, it is possible to solve this approximation analytically, and also to obtain corrections to it representing the more complicated cases discussed above [12].

2 Results

Temporal transients. We obtained Ca^{2+}transients for a large variety of parameter values. Figure 1 shows curves differing in the choices of peak influx current and also approximation involved. Source timescales varied from unrealistically fast ($\sim$ 90ms) up to around 300 ms (the faster cases were chosen to provide upper bounds on nonequilibrium effects). Several results could be deduced. First, in no cases were the assumptions of equilibrium unequivocally verified. Numerical computations of all timescales involved show that for relevant values of the parameters the system was on the borderline of equilibrium. These computations involved estimating the entire chemical kinetic system, including the effects of different reactions on each other: see [2, 12]. They were themselves more reliable for smaller current sources, since they rely on an assumption of small deviations from resting $[Ca^{2+}]$. For the circumstances considered, the chemical equilibrium approximation did give reasonable results, which are valuable in characterizing experimental data. It seems generally best to assume that peaks may be subject to errors of a few percent, particularly for low dye concentrations and large Ca^{2+}influxes —in other words, the same conditions when saturation is a danger.

Nonequilibrium effects decrease as the timescale of the influx becomes longer. This is so because the calcium to be split among the different reactions becomes available more gradually. As the source gets larger, this variation in time becomes less noticeable, because then the supply of free calcium available to slower buffers is dominated by the dynamics of the source itself, not by calcium liberated by faster buffers.

Other points found include the following. Times to peak do not increase greatly with influx time course (indeed, their growth is slower as the time course increases, which would suggest a fractional power dependence: analytically, this turns out to be true to leading order). Second, the simple linear approximation is very poor (although it does predict times to peak reasonably well). This is true

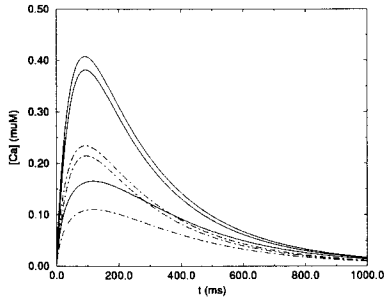

Fig. 1. $[Ca^{2+}]$ temporal transients at $x = 0$ with $\tau_0 = 300$ms source: comparison between different approximations. (*Solid lines*) $J_0 = 3.0\mu$M ms^{-1}, (*dashed-dotted lines*) $J_0 = 2.0\mu$M ms^{-1}. For each set, (*largest transient to smallest*) correspond to full equations, equilibrium approx., linear approx. Common parameters: Γ =2.5 ms^{-1}, F_T = 50 μm

even for the smaller $J_0 = 2\mu$M ms^{-1} transients, when the peaks never exceed the dye's dissociation constant. Third, observation of dye-bound Ca^{2+}transients (not shown) indicates that these data are far away from the saturated limit: there is no [FCa] peak suppression. Therefore no a priori linear approximation works well.

Discrepancies between the equilibrium approximation and its simple linear limit can be traced to the choice of a constant limit for the capacity, which is clearly inadequately large over the transient's duration. (The peak decreases with increasing capacity —see below—, and consequently is grossly underestimated for this single reason.) One would then hope for an interpolative scheme capable of reproducing the data better than the linear approximation, but offering the simplicity of a constant capacity (i.e. one independent of concentration but averaged over the transient's extent). It turns out that such a scheme is indeed possible and involves an "effective capacity" that can be obtained by direct fit to the full set of equations, or alternatively by substituting a constant, averaged value of $[Ca^{2+}]$. Figure 1 shows that the scheme makes sense. Similar definitions have already been used in the literature [5]. In data interpretation the use of simple equilibrium models often requires an "incremental capacity" that interpolates between peak and resting $[Ca^{2+}]$ [6, 8, 11].

Spatial spread. What determines the spread of calcium? In the regime where buffering can be assumed to equilibrate locally, diffusion is controlled by the $[Ca^{2+}]$-dependent effective parameter (diffusion "constant")

$$D_{eff} = \frac{D_{\mathrm{Ca}} + \kappa_{\mathrm{B}} D_{\mathrm{B}} + \kappa_{\mathrm{F}} D_{\mathrm{F}}}{1 + \kappa_{\mathrm{B}} + \kappa_{\mathrm{F}}}. \tag{4}$$

At $F_T = 0$, this is $D_{eff} = (D_{\mathrm{Ca}} + \kappa_{\mathrm{B}} D_{\mathrm{B}})/\kappa_{\mathrm{B}}$. The endogenous buffer is essentially immobile ($D_{\mathrm{B}} \approx 0$) and its capacity is close to being constant due to low affinity

($\kappa_B \approx B_T/K_D^B$). Consequently its main effect on Ca^{2+}diffusion is to reduce it by a factor equal to the buffer's capacity. Since this capacity is estimated to be of the order of $100 - 200$, Ca^{2+}dynamics in the natural state are rather slow. What this reflects is that free $Ca^{2+}$is subject to a buffering process that is in competition with diffusion, the net effect of which is that it takes longer for the average Ca^{2+}ion to spread away from the source.

When the dye is added, (1) the effective diffusion constant is altered, (2) steady-state calcium gradients are no longer possible even for a steady-state source, i.e. $Ca^{2+}$is redistributed locally. Spatial changes in $[Ca^{2+}]$ will be washed out by the availability of a pool of circulating, unbound dye. (This buffer's mobility implies that it is not depleted at any position in particular, notably close to the source.) The upshot is that any localization effects due to the immobile buffers' action are substantially diminished. Because fluorophores are high-affinity buffers, the dependence of D_{eff} on calcium concentration is very marked in their presence. (The dye capacity's dependence on $[Ca^{2+}]$ cannot usually be neglected, in contrast to that of the low-affinity buffer's.) For these reasons, regions starting with a high Ca^{2+}concentration will see it diffuse away.

The diffusion constant increases with κ_F at a relatively fast rate to begin with, but eventually reaches an absolute limit equal to D_F: at high loading, the dye binds more calcium than the endogenous buffer. This means that it is actually easier to reach reliable conclusions about spatial calcium in a regime of *high loading* than in a regime of low to medium loading, since in the latter case the spread is much more sensitive to the specific value of the capacity: minute changes in dye concentration can alter Ca^{2+}mobility quite heavily. (The capacity is unknown a priori anyway, since being in a low-loading regime automatically means that nonlinearity and saturation are much more easily reached.) Close to the high-fluorophore limit, the effective diffusion constant's dependence is simple:

$$D_{eff} \approx D_F - \frac{1 + \kappa_B}{\kappa_F}. \tag{5}$$

Figure 2 illustrates these points. At high dye loading, the calcium profile reaches a maximum width and then does not spread any more, although one can observe that for high F_T there is a relatively wide, but small tail. In our simulations we never observed profiles wider than around 5μm; these data suggest that $Ca^{2+}$is probably localized to within a scale of $2 - 3\mu$m, a result consistent with other recent experimental data for hippocampal dendrites [9]. Such localization is the result of the competition between buffer-limited diffusion, Ca^{2+}extrusion and clearance: no other mechanisms are necessary. Although dendritic spines seem to function as chemical compartments (see e.g. [14]), from this result they do not appear critical to the localization of calcium transients and thus to chemical synapse specificity. Note that these results were obtained with a homogeneous buffer distribution, and that increased localization would be possible, if necessary, by simply distributing the buffer differentially —with no need for the complication of spines.

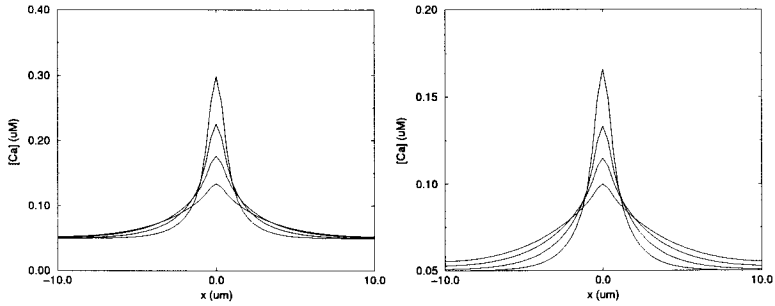

Fig. 2. Spatial $[Ca^{2+}]$ profiles at $t = 300$ ms (*left*) and $t = 500$ ms (*right*), for J_0= 3.0 μM ms^{-1}, τ_0 =300 ms. (*Highest to lowest*) $F_T = 20\mu$M, $F_T = 50\mu$M, $F_T = 100\mu$M, $F_T = 200\mu$M. Other parameters as per figure 1

In spite of the inadequacies of the linear limit, it can estimate $[Ca^{2+}]$ profile widths rather well. Profile edges of course have low concentration, i.e. are in the natural range of applicability for the linear approximation. An immediate corollary is that spatial fluorescence tails proportional to [FCa] may be good markers of $[Ca^{2+}]$, because the relationship at the tail is close to linear: see below for further discussion on how Ca^{2+}peaks can be estimated using the profiles' tails.

Solution in linear approximation. As mentioned, one can produce an analytical solution valid in linear approximation, including the case when an "effective" value of the capacity can be fit to the calcium transients that verify the full set of equations. The equation to be solved can be written as

$$\frac{\partial c}{\partial r} = \delta \frac{\partial^2 c}{\partial s^2} - \gamma(c-1) + f(s)\exp(-r/\tau). \tag{6}$$

under the assumption (discussed earlier) that the source function's temporal dependence is exponential, $\exp(-t/\tau_0)$. This form of the equation involves a transformation into adimensional "natural" variables,

$$c \equiv \frac{C}{C_0},\ r \equiv t\frac{J_0}{\bar{\kappa} C_0},\ s \equiv x\sqrt{\frac{J_0}{\bar{\kappa} D_{\mathrm{Ca}} C_0}},\ \tau = \frac{r\tau_0}{t},\ \gamma \equiv \Gamma\frac{C_0}{J_0},\ \delta \equiv \frac{D_T}{D_{\mathrm{Ca}}\bar{\kappa}}. \tag{7}$$

The conversion factors provide a natural set of spatial and temporal scales for the problem, which can be compared to the chemical equilibration time course. The result is that, as anticipated, chemical kinetics unfold on a timescale faster but similar to that of diffusion (whose values are around $5 - 10$ms).

Some quantitative features of equation 6 can be seen without any need for further manipulations. For instance, the parameter that most determines transient sizes is (not surprisingly) J_0, or more correctly J_0/C_0. That the dependence is always in this form can be seen directly from the equation. The inverse problem

of attempting to back-calculate NMDA current values from a given transient curve is thus only well-defined to the degree that one can estimate the resting $[Ca^{2+}]$, or measure it separately. Because experimental estimates of C_0 are usually not separate from fluorescence measurements, this implies a problem in estimating peak current. We plotted [12] $[Ca^{2+}]$ and [FCa] peaks across a wide range of peak currents and decay times, confirming that the dependence on J_0 was much more pronounced than on τ_0. Since the total number of Ca^{2+}ions is proportional to the product $J_0 \times \tau_0$, this dependence is then not merely on the total ionic influx, but on how quickly it is distributed.

As for the equation's solution, given $a^2 \equiv 1/\delta(\gamma - 1/\tau)$, one obtains (for $a^2 > 0$)

$$c(s,r) = \frac{\exp(-r/\tau)}{4\delta a} \int_{-\infty}^{+\infty} d\eta f(\eta - s) \tag{8}$$
$$\times \left[2e^{-a|\eta|} - e^{a\eta}\mathrm{erfc}\left(a\sqrt{\delta r} + \frac{\eta}{\sqrt{4\delta r}} \right) - e^{-a\eta}\mathrm{erfc}\left(a\sqrt{\delta r} - \frac{\eta}{\sqrt{4\delta r}} \right) \right].$$

For $a^2 < 0$ one finds a similar, but apparently complex solution whose imaginary part cancels out; for $a = 0$, a simplified version of the solution obtains (see [12]).

Estimating calcium signals from fluorescence tails. The equilibrium relationship between [FCa] and $[Ca^{2+}]$ can be inverted to yield estimates of calcium concentration based on fluorescence intensity. However, away from the region where binding is approximately linear, and in particular close to the saturated regime when there is enough calcium to induce [FCa]$\rightarrow F_T$, the process is complicated considerably. Data are of course corrupted by noise, and by uncertainty concerning parameter values; under these conditions, it is very difficult to interpret fluorescence as an indicator of Ca^{2+}concentration. This is a particular problem for $[Ca^{2+}]$ peaks and quantities related to them (such as times to peak), since they involve the regions of the transients most prone to saturation.

However, one can imagine the alternative of using [FCa] tails as an indicator of $[Ca^{2+}]$ peaks. We carried this out with calcium profiles from our model and checked whether these quantities could safely be considered to satisfy quasi-linear relationships. We varied the influx characteristics (J_0, τ_0) over a wide range, for fixed values of the other model parameters. We then plotted peak-tail relationships for both $[Ca^{2+}]$ and [FCa], and the consequent relationships between [FCa] peaks and $[Ca^{2+}]$ peaks, and [FCa] tails and $[Ca^{2+}]$ peaks. As the influx parameters varied, we shifted from a region close to the linear limit to a region with clear [FCa] saturation. Tail values were computed by taking integrals over the later areas of the curves, a more robust measure than evaluation at a single, arbitrary point. Choosing the integration limits has to be done contemplating a balance between the need not to take into account regions highly liable to saturation (i.e. too close to the "suppressed" or saturated peak), and on the other hand the need to prevent extreme sensitivity to noise and loss in resolution at the tail, i.e. to conserve a large enough signal. This decision must be made ad hoc for each trial dataset.

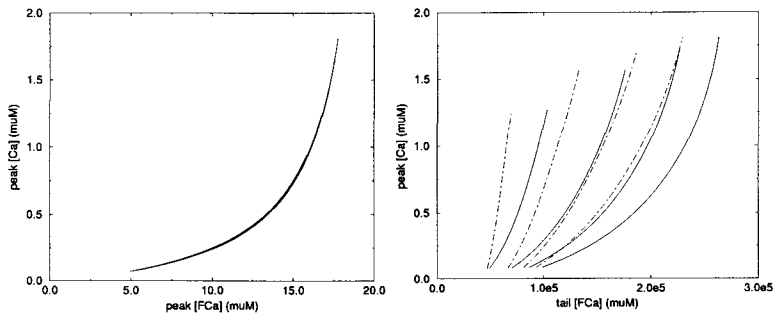

Fig. 3. (*Left*) $[Ca^{2+}]$ peaks versus [FCa] peaks. Saturation is clear. (*Right*) $[Ca^{2+}]$ peaks versus [FCa] tails. (*Rightmost curves to leftmost*) τ_0 = 400ms to τ_0 = 100ms. (*Solid lines*) lower and upper cutoffs equal to 4× time to peak and 6× t.t.p.; (*dot-dashed lines*) cutoffs equal to 6× t.t.p. and 8× t.t.p. All other data as per previous figures

Figure 3 shows the resolution gained by using [FCa] tails instead of peaks, and also the delicate tuning that must be carried out. Two choices of cutoffs were used, with lower and upper values set respectively at 4× time to peak (t.t.p.), 6× t.t.p.; and 6× t.t.p., 8× t.t.p. Curves obtained with the higher choice of cutoffs (the curves most to the left in part (b) of the figure) show almost no saturation and a quasilinear dependence of $[Ca^{2+}]$ peaks on [FCa] tails, but at the cost of very small slopes (i.e. with a very low signal to noise ratio). These results suggest that using fluorescence tails instead of peaks as a method of estimating $[Ca^{2+}]$ peaks does make sense, although the successive steps involved in going from one measure to another are themselves nonlinear. We have not yet carried out a detailed analysis of the method for particular experimental instances.

References

1. Denk, W., Yuste, R., Svoboda, K., and Tank, D.W., *Curr. Opin. Neurobiol.* **6** (1996): 372.
2. Sabatini, B.R., and Regehr, W.G., *Biophys. J.* **74** (1998): 1549.
3. Wagner, J., and Keizer, J., *Biophys. J.* **67** (1994): 447.
4. Smith, G.D., Wagner, J., and Keizer, J., *Biophys. J.* **70** (1996): 2527.
5. Kupferman, R., Mitra, P.P., Hohenberg, P.C., and Wang, S.S.-H., *Biophys. J.* **72** (1997): 2430.
6. Neher, E., and Augustine, G.J., *J. Physiol.* **450** (1992): 273.
7. Zhou, Z., and Neher, E., *J. Physiol.* **469** (1993): 245.
8. Helmchen, F., Imoto, K., and Sakmann, B., *Biophys. J.* **70** (1996): 1069.
9. Murthy, V.N., Sejnowski, T.J., and Stevens, C.F., personal communication.
10. Sala, F., and Hernández-Cruz, A., *Biophys. J.* **57** (1990): 313.
11. Markram, H., Roth, A., and Helmchen, F., *J. Comp. Neurosci.* **5** (1998): 331.
12. Mainen, Z.F., Maravall, M., and Svoboda, K., in preparation.
13. Hines, M.L., and Carnevale, N.T., *Neural Comput.* **9** (1997): 1179.
14. Yuste, R., and Denk, W., *Nature* **375** (1995): 682.